AIP Journal of Applied Physics

Spin noise amplification and giant noise in optical microcavity

I. I. Ryzhov, S. V. Poltavtsev, G. G. Kozlov, A. V. Kavokin, P. V. Lagoudakis, and V. S. Zapasskii

Citation: Journal of Applied Physics **117**, 224305 (2015); doi: 10.1063/1.4922405
View online: http://dx.doi.org/10.1063/1.4922405
View Table of Contents: http://scitation.aip.org/content/aip/journal/jap/117/22?ver=pdfcov
Published by the AIP Publishing

JOURNAL OF APPLIED PHYSICS **117**, 224305 (2015)

Spin noise amplification and giant noise in optical microcavity

I. I. Ryzhov,[1] S. V. Poltavtsev,[1] G. G. Kozlov,[1] A. V. Kavokin,[2,1] P. V. Lagoudakis,[2] and V. S. Zapasskii[1]
[1]*Spin-Optics Laboratory, St. Petersburg State University, 198504 St. Petersburg, Russia*
[2]*Department of Physics & Astronomy, University of Southampton, Southampton SO17 1BJ, United Kingdom*

(Received 17 April 2015; accepted 29 May 2015; published online 11 June 2015)

When studying the spin-noise-induced fluctuations of Kerr rotation in a quantum-well microcavity, we have found a dramatic increase of the noise signal (by more than two orders of magnitude) in the vicinity of anti-crossing of the polariton branches. The effect is explained by nonlinear optical instability of the microcavity giving rise to the light-power-controlled amplification of the polarization noise signal. In the framework of the developed model of built-in amplifier, we also interpret the nontrivial spectral and intensity-related properties of the observed noise signal below the region of anti-crossing of polariton branches. The discovered effect of optically controllable amplification of broadband polarization signals in microcavities in the regime of optical instability may be of interest for detecting weak oscillations of optical anisotropy in fundamental research and for other applications in optical information processing. *© 2015 AIP Publishing LLC.*
[http://dx.doi.org/10.1063/1.4922405]

I. INTRODUCTION

Studies of spin fluctuations by means of optical polarimetry, commonly referred to as spin noise spectroscopy, are becoming increasingly popular during the recent years.[1] Spin fluctuations in a paramagnet, as has been first demonstrated in Ref. 2, give rise to fluctuations of its gyrotropy, which can be detected by means of the optical polarimetry as a noise of probe beam polarization plane rotation. Spectrum of the noise thus observed, in conformity with the fluctuation-dissipation theorem, reflects frequency dependence of the magnetic susceptibility of the medium and, in the simplest case of magnetic field aligned across the light beam propagation, is represented by a Lorentzian centered at Larmor frequency and having the width controlled by the spin dephasing rate. Since the samples investigated in real experiments are, as a rule, transparent for the probe beam, the spin noise spectroscopy is considered to be a nonperturbative method of measuring magnetic susceptibility and, thus, studying spin dynamics.

The growing popularity of spin noise spectroscopy during the last years is related, in particular, to appearance of fast Fourier transform (FFT) spectrum analyzers, which made it possible to successfully employ this technique, previously applicable mainly to atomic systems,[2–4] for studying semiconductor structures in the range of radiofrequencies.[5,6] A number of recent refinements proposed in Refs. 7 and 8 made it possible to additionally increase sensitivity of the measurements. Besides, methods of spin noise detection, utilizing output emission of mode-locked lasers for probing the medium, proposed and realized in Refs. 9–11 made it possible to extend the frequency range of the spin noise spectroscopy up to terahertz frequencies. Specific feature of the present-day spin noise spectroscopy is that it mainly deals with low-dimensional semiconductor structures (quantum wells (QWs), quantum wires, quantum dots), which are considered to be most promising objects for applications in the future information technologies. As examples of this trend may serve the recent publications.[12–15] By placing such objects into a inter-mirror gap of a high-Q Bragg microcavity and observing polarization noise of a probe beam reflected from (or transmitted through) such a compound system, one can strongly (by several orders of magnitude) enhance the noise signal.[15] This gives promise that the spin noise spectroscopy of semiconductor nanostructures in microcavities will become an important self-contained part of the modern experimental physics.[16]

In this paper, we study properties of the Kerr rotation noise of a light beam reflected from a semiconductor AlGaAs Bragg λ-microcavity with a GaAs QW in its inter-mirror gap (the cavity). The structure under study was graded to make possible detection of the noise signal of Kerr rotation at different detunings between photon mode of the cavity and the QW excitons. For the region of the sample where the frequency of the microcavity photon mode is substantially lower than that of the QW exciton (the region of negative detuning), the Kerr rotation noise spectrum, as was found in Ref. 15, exhibits a nontrivial bimodal shape. When passing to regions of the sample, where the photon mode frequency approaches to that of the QW excitons (the region of anti-crossing), we observed enhancement of the noise signal by several hundred times (the *giant noise*). In this paper, we show that these specific properties of the noise signal can be explained by the nonlinear instability of the microcavity accompanied by a critical increase of sensitivity of the microcavity reflectivity to fluctuations of the intracavity refractive index. The discovered effect can be used to detect weak signals of oscillating optical anisotropy in fundamental and applied research.

The paper is organized as follows. In Section II, we describe the experimental set-up, the sample under study, and results of the measurements. In Sec. III, we formulate hypothesis of the built-in amplifier, which allows us to

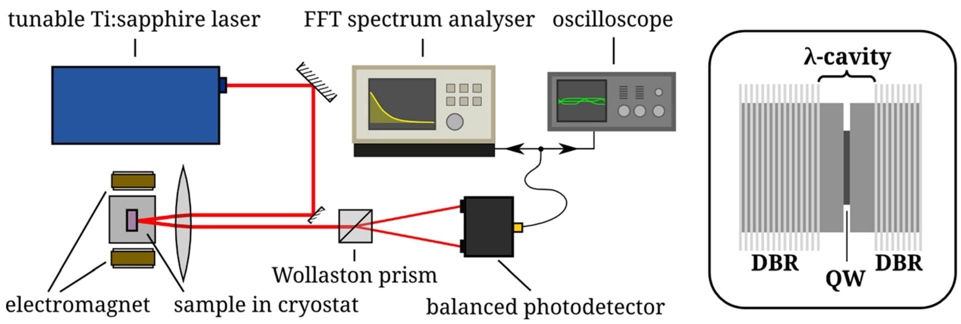

FIG. 1. Experimental setup. Structure of the sample is shown schematically in the inset.

explain mechanism of the giant noise and to derive a formula describing the bimodal noise spectrum at negative detuning. In Sec. IV, we consider experimental study of response of the microcavity to an external high-frequency electromagnetic field, to confirm optical nonlinearity of the effect. In Sec. V, we present a simple model of a nonlinear instable cavity and provide qualitative explanation of all the noise properties of the sample. In Conclusions, we briefly summarize the results of this work.

II. EXPERIMENTAL

We studied the sample used in Refs. 15 and 17, representing a planar Bragg λ-microcavity with a GaAs QW (102/200/102 Å AlAs/GaAs/AlAs) in the center of the inter-mirror gap. The experiment was performed using the set-up for observation of the Kerr-rotation noise, described in detail in Ref. 15 (Fig. 1). As a probe, we used a linearly polarized beam of a tunable Ti:sapphire laser, at normal incidence, focused on the sample in a spot $\sim 20\,\mu$m in diameter. For spin density $n_e \sim 10^{10}$ sm^{-2} mentioned in Ref. 15, we estimate the number of spins contributing to our noise signal to be $\sim 5 \times 10^4$. The sample placed into a magneto-optical module of a closed-cycle cryostat Montana was cooled down to 3–8 K. The light beam reflected from the sample was directed to the polarimetric receiver consisted of a polarizing beam splitter (Wollaston prism) and a broadband ($\Delta\nu = 200$ MHz) balanced photodetector. Magnetization fluctuations in the inter-mirror gap of the microcavity (related to the spin noise of free carriers or excitons in the QW) caused polarization fluctuations in the reflected beam giving rise the noise signal at the exit of the photodetector. The wavelength of the probe beam was tuned to obtain the greatest noise signal.

A standard spin noise experiment implies measuring radiofrequency spectrum of this signal as a function of the applied transverse magnetic field. Such a spectrum is detected by a FFT spectrum analyzer and, as was mentioned in Introduction, in the simplest case, has a Lorentzian shape with its peak shifting in proportion with the applied magnetic field.

From the reflectivity spectra presented in Ref. 17, one can see that spectral position of the photon mode of the microcavity strongly depends on spatial coordinate on the sample. In this connection, it is expedient to specify three regions of the sample. (i) The region of negative detuning, where the photon mode frequency is lower than those of excitons in the QW. Taking the edge of the sample for a starting point, this region corresponds to the spatial interval from 0 to 300 μm. (ii) The region of anti-crossing of the polariton branches, where the photon mode frequency intersects the QW exciton frequencies (300–900 μm). (iii) The region of positive detuning, where the photon mode frequency becomes higher than those of the QW excitons (above 900 μm). In this region, the noise signal is strongly suppressed, because the asymmetric microcavity used in these experiments is operating, at this detuning, in the post-critical regime.[18] Note that the noise signal detected in Ref. 18 was observed under red irradiation, which is not the case for our present experiments. Properties of the noise signals in the first two regions substantially differ and are described in more detail below.

Region of negative detuning. The Kerr-rotation noise power spectra obtained in this region of the sample at different magnetic fields are presented in Fig. 2 (noisy curves). A nontrivial property of the spectra is their bimodal shape in nonzero magnetic fields: along with a usual magnetic peak at Larmor frequency shifting in magnetic field with a g-factor of 0.35, the spectra show a distinct "nonmagnetic" peak in the vicinity of zero frequency. The amplitude of this peak decreases with increasing magnetic field, while its spectral position remains the same.

Dependence of the noise power on the probe beam intensity was found to differ noticeably from quadratic, thus indicating a contribution of optical nonlinearity. The most pronounced nonlinear behavior was revealed by the nonmagnetic peak of the noise spectra, whose relative amplitude

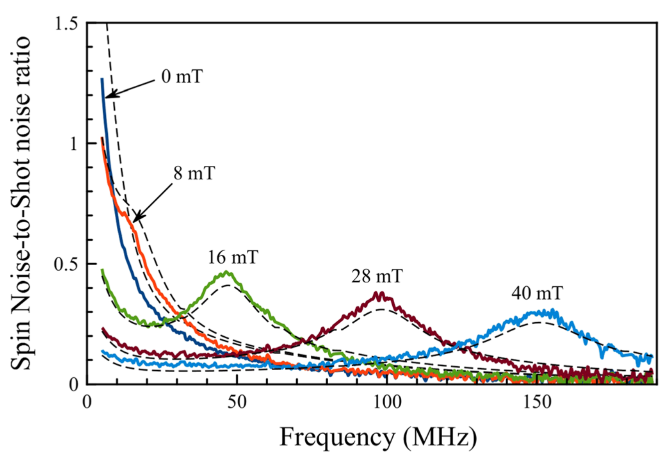

FIG. 2. The noise spectra in the region of negative detuning at different magnetic fields. The noisy curves—experiment, smooth curves—fitting by Eq. (1).

rapidly decreased with decreasing light intensity. The magnitude of the noise signal in this region of the sample was of the order of shot-noise power of the probe beam, whose intensity, in our experiments, was about 1 mW.

Region of anti-crossing of the polariton branches. Our experiments have shown that, by moving the spot of the focused probe beam in this region of the sample, we could find the points of *giant noise* where the noise signal amplitude, in zero magnetic field, exceeded its amplitude in the region of negative detuning by several hundred times. The giant noise spectrum had the shape of a peak at zero frequency, ∼10–20 MHz wide, with its amplitude decreasing with magnetic field (Fig. 3(a)). As the probe beam intensity increased, the amplitude of the giant noise exhibited an essentially nonlinear behavior: a steep growth at moderate intensities was replaced by a decrease at the intensities exceeding 1 mW (Fig. 3(b)). When detecting the above spectra, the spectrum analyzer was adjusted to detect the spectra starting from 5 MHz. A direct study of the output signal of the balanced detector at low frequencies, using an oscilloscope, has shown that the regime of giant noise was accompanied by strong chaotic polarization oscillations at the frequencies of 1–50 kHz. The above instable behavior in the light polarization was observed at sufficiently high intensities of the probe beam. A similar behavior was demonstrated by the probe beam *intensity*.

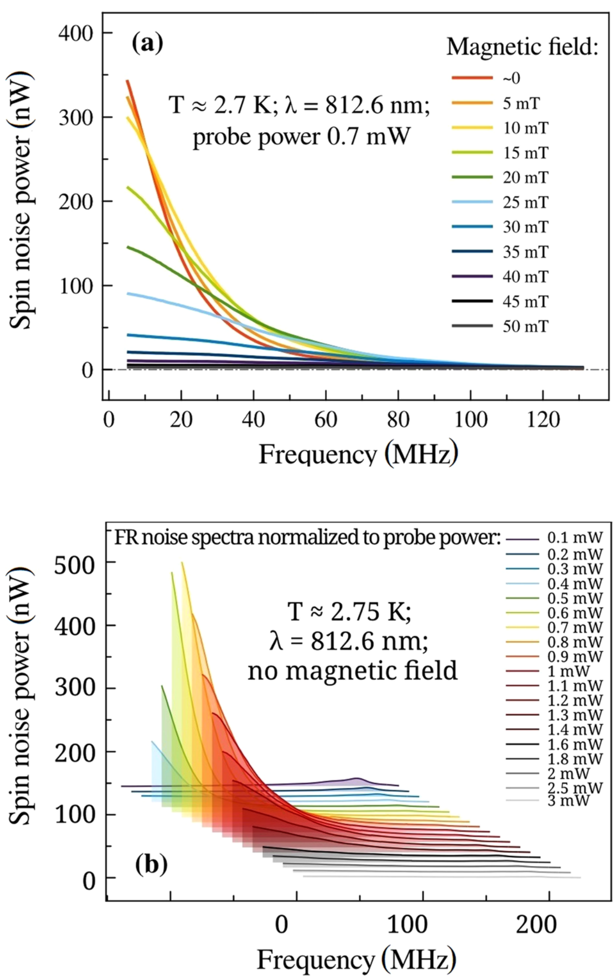

FIG. 3. (a) The giant noise spectra at zero magnetic field for different probe beam intensities. (b) The giant noise spectra at different magnetic fields.

III. HYPOTHESIS OF THE BUILT-IN AMPLIFIER

The results presented in Sec. II unambiguously indicate crucial role of optical nonlinearity in the formation of the Kerr-rotation noise signals observed in our experiments. Nonlinear behavior of optical cavities with nonlinear absorbers is well known and has been studied earlier in great detail.[19–21] Special attention has been paid to semiconductor microcavities in the strong-coupling regime, with the nonlinearity resulting in the optical bistability under quasi-resonant excitation of the lower exciton-polariton branch.[22,23] In this respect, the behavior of our microcavity does not look surprising, because there are at least two reasons why the optical field strength in the inter-mirror gap may exceed by many orders of magnitude the field strength in the probe beam: a sharp focusing of the beam on the surface of the sample and resonant enhancement of the field strength in the high-Q microcavity. We can judge about the scale of the nonlinearity from the measured spectra of reflectivity at different regions of the sample with intensities of the probe beam differed by an order of magnitude (Fig. 4). The measurements of the reflectivity spectra were performed under the same conditions as the measurements of the noise spectra. It is seen from the figure that dependence of the reflectivity spectrum on the probe beam intensity is distinctly revealed even in the region of negative detuning and becomes dramatic in the region of anti-crossing of the polariton branches where the giant noise is observed. This behavior of the reflectivity spectra allows us to suggest the following schematic explanation of the oscillatory instability of the microcavity described in the end of Sec. II. When the resonant light beam is turned on, the light field amplitude in the microcavity starts to build-up. Due to the nonlinearity of the medium in the inter-mirror gap (resulted, e.g., from saturation of the QW-exciton

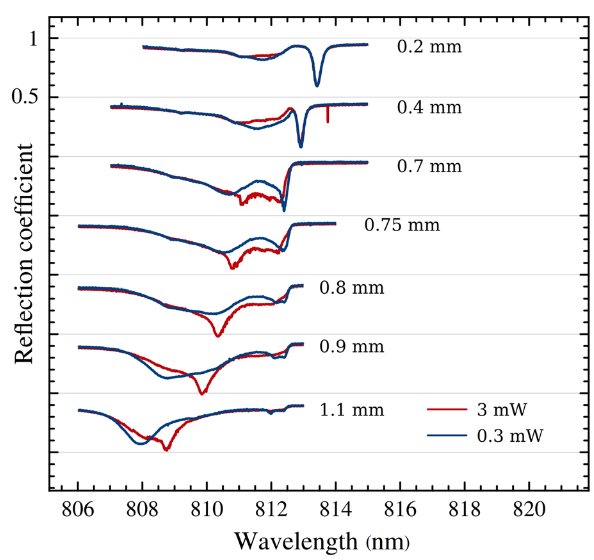

FIG. 4. Reflectivity spectra of the QW microcavity for different relative positions of the photon mode and QW exciton resonances. The spectra 0–300 μm correspond to the region of negative detuning and the spectra 300–900 μm to the region of anti-crossing of the polariton branches. The measurements were performed for two laser beam intensities: 3 mW (red curves) and 0.3 mW (blue curves).

susceptibility), the microcavity comes out of resonance with the light field. As a result, the amplitude of the optical field in the microcavity decreases, and it again comes back to the resonance, the field inside it again increases, and so on. Such a mechanism of self-excitation with auto-oscillations of the field amplitude should reveal a threshold-type behavior with respect to the light intensity. It is well known that the systems of this kind, in the vicinity of the self-excitation threshold, become highly sensitive to variations of their parameters. This is why it is natural to expect that sensitivity of the reflection coefficient of the nonlinear microcavity to fluctuations of its optical properties may strongly increase when the light beam intensity approaches the self-excitation threshold. This is supported by the analysis of a simple model presented in Sec. IV.

In our opinion, the giant noise arises in the region of strong optical nonlinearity due to pre-threshold increase of sensitivity of the cavity reflectivity to spin fluctuations (fluctuations of gyrotropy in its intermirror gap).

Based on this hypothesis, the Kerr-rotation noise signal S observed in our experiments can be represented in the form $S = (\xi + 1)M$, where M is the noise signal that would have been observed in the optically linear microcavity and ξ is the factor that accounts for the nonlinearity-related amplification of polarimetric response of the cavity. In accordance with the aforesaid, the factor ξ should depend on the probe beam intensity $\xi = \xi(I)$, with $\xi(0) = 0$, while with approaching I to its threshold value I_c, it should strongly increase, $\xi(I_c) \gg 1$. Thus, we can say that the above nonlinearity turns the microcavity into an effective built-in amplifier of its ac gyrotropy with the gain factor ξ controlled by the light intensity. Since, in our experiments, we observe *frequency* dependence of the noise power, we should take into account that the gain factor ξ may depend on frequency ω: $\xi = \xi(I, \omega)$.

As was noted in Sec. II, the noise signal from the sample shows a noticeable nonlinearity even in the region of negative detuning, where no giant noise is observed. Now, we will show that the hypothesis of the built-in amplifier can explain, in a natural way, the presence of nonmagnetic peak in the noise power spectrum, described in the Sec. II.[25] We assume that the frequency dependence of the gain factor ξ has the shape of a Lorentzian[26] with the halfwidth Δ centered at zero frequency

$$\xi(I,\omega) = \xi_0(I)\Delta\pi\mathcal{L}(\Delta,\omega),$$

where $\mathcal{L}(\Delta,\omega) \equiv \pi^{-1}\Delta/[\Delta^2+\omega^2]$ and $\xi_0 = \xi(I, 0)$. Then, in accordance with the hypothesis of the built-in amplifier, for the noise power spectrum observed in our experiment, we can write the following equation:

$$S(\omega) = (\xi_0(I)\pi\Delta\,\mathcal{L}(\Delta,\omega)+1)\overbrace{C[\mathcal{L}(\Delta_e+kH,\omega-g\beta H/\hbar)+\mathcal{L}(\Delta_e+kH,\omega+g\beta H/\hbar)]I^2}^{M}. \tag{1}$$

Here, the factor in square brackets corresponds to the classical spectrum of spin noise in the magnetic field H (Lorentzian peak with the halfwidth Δ_e centered at the Larmor frequency $g\beta H/\hbar$); the factor I^2 takes into account dependence of the observed signal on the probe beam intensity for linear regime of the microcavity (it is quadratic because we detect *power* of the noise signal); the parameter k takes into account a noticeable broadening of the noise spectrum with magnetic field observed in our experiments (it can be explained by a spread of g-factors of the spins contributing into the noise signal); and C is the proportionality factor controlled by parameters of the photodetector (quantum yield, load resistor, etc.), whose weak frequency dependence is ignored. The results of fitting of the experimental noise spectra using Eq. (1) are presented in Fig. 2 (smooth curves). The values of parameters obtained in this fitting are: $\xi_0 = 2.5$, $\Delta = 2\pi \times 7\,\mathrm{MHz}$, $\Delta_e = 2\pi \times 20\,\mathrm{MHz}$, $k = 0.3\,\mathrm{MHz/mT}$, and $|g| = 0.35$. As expected, the gain factor ξ_0 proved to be small, i.e., optical nonlinearity in the considered region of negative detuning is not pronounced. The fact that, in this case, $\xi_0 \sim 2$ is reflected in the bimodal shape of the observed noise spectrum: the *nonmagnetic* peak corresponding to the low-frequency components of the spin noise amplified by the built-in amplifier and the *magnetic* peak at Larmor frequency have comparable amplitudes. As the probe beam intensity decreases, the gain factor ξ_0 (controlled by the optical nonlinearity) decreases, and the nonmagnetic peak of the noise spectrum is being suppressed.

When passing to the region of the sample with strong optical nonlinearity (the region of anti-crossing of the polariton branches), where the giant noise is observed, the gain factor ξ_0 increases and eventually reaches several hundreds. In accordance with Eq. (1), the observed signal, in this case, represents only the spin noise amplified by the built-in amplifier: the entity in parentheses can be neglected. Since the efficient amplification occurs only in the region of near-zero frequencies, with a width of $\sim\Delta$, at points of the giant noise we observe only low-frequency components of the spin noise with frequencies $\omega < \Delta$, and the giant noise spectrum acquires a monomodal shape (Fig. 3). When the magnetic field is turned on, amplitudes of these components decrease because the peak of the spin noise spectrum (at Larmor frequency) shifts towards higher frequencies. This explains a decrease of the giant noise amplitude with magnetic field.

IV. EXPERIMENTS WITH A REGULAR FIELD-INDUCED PERTURBATION OF THE MICROCAVITY

In conformity with the hypothesis of the built-in amplifier formulated in Sec. III, reflectivity of the *nonlinear* microcavity can be much more sensitive to intracavity changes of optical susceptibility than the linear microcavity.

In the experiments described above, variations of optical susceptibility of the inter-mirror gap were related to *spontaneous* spin fluctuations. The effect of amplification, however, should not depend on the source of these variations and, in particular, should lead to amplification of polarimetric response of the microcavity to a regular ac magnetic (or electric) field created by external sources. In this case, variation of optical susceptibility (gyrotropy or linear birefringence) of the medium in the inter-mirror gap is related to the Faraday (Pockels) effect, while the effect of the built-in amplifier should manifest itself in an essentially nonlinear dependence of the polarimetric response of the microcavity on the probe beam intensity. Our experimental observation of such a response to a high-frequency electromagnetic field created by an oscillatory circuit mounted on the sample has shown that the above nonlinear dependence took place indeed. The experiments were performed in the following way. A coil of the oscillatory circuit (15 turns 10 mm in diameter) was placed in front of the sample so that its magnetic field was directed perpendicular to the plane of the sample (along the incident beam). A capacitor of the circuit was chosen to provide its resonant frequency of about 15 MHz. The circuit was resonantly excited by a pick-up coil fed by a high-frequency oscillator. Under these conditions, a narrow peak at the frequency ∼15 MHz was seen in the spectrum of the photodetector output signal. This peak displayed a resonant behaviour (with respect to the light wavelength), which showed that it is related to modulation of optical susceptibility of the medium in the inter-mirror gap of the microcavity. In the region of the sample corresponding to the giant noise, the magnitude of this peak substantially varied with the spot on the sample. However, dependence of its amplitude on the probe beam intensity was always nonlinear (Fig. 5). In some places of the sample, this dependence was even nonmonotonic. In spite of the fact that these results are not yet quite systematic, they unambiguously indicate a decisive role of nonlinearity of the microcavity in formation of its polarimetric response. Note that this response revealed a noticeable nonlinear behavior even in the region of negative detuning (where no giant noise was observed), which confirms the above mechanism of formation of the nonmagnetic component of the noise spectrum in this region.

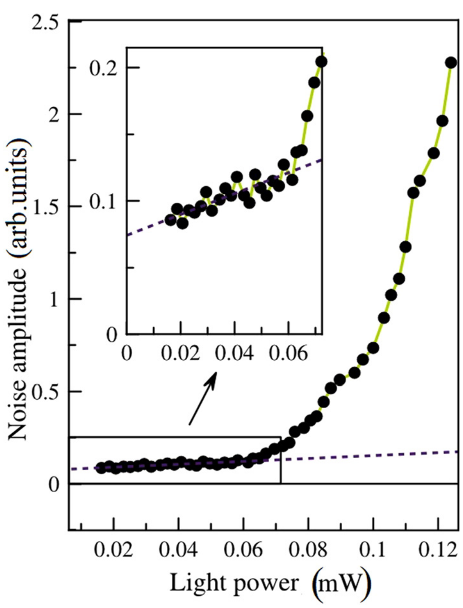

FIG. 5. Experimental dependence of amplitude of the field-induced response of the microcavity on the probe beam intensity.

In our experiments, modulation of the optical susceptibility of the medium in the inter-mirror gap was, most likely, controlled by the electro-optical Pockels effect (inherent in GaAs). The effect of magnetic field created on the sample by the coil of the oscillatory circuit was relatively weak, which was evidenced by weak dependence of the polarimetric response amplitude on the coil orientation: it remained practically the same with the coil axis aligned along the plane of the sample.

V. MODEL OF NONLINEAR OSCILLATOR

Development of a detained model of nonlinear cavity (with allowance for a particular mechanism of the optical nonlinearity, spatial nonuniformity of the microcavity, and profile of the focused probe beam) at this stage of the research seems premature. The task of this section is to build the simplest model of a nonlinear cavity demonstrating, at the self-excitation threshold, a manifold increase of sensitivity of the cavity reflectivity to variations of refractive index of the medium in the inter-mirror gap. In spite of the fact that, in our experiments, we examined *polarization properties* of the reflected beam (rather than pure reflectivity), the model presented below describes, in our opinion, the most important qualitative properties of a real cavity and, to a great extent, justifies the assumptions made above upon formulation of the built-in amplifier hypothesis.

Let us put into correspondence with the microcavity an oscillator, with the resonant frequency ω_0 and spectral width of the resonance $\Delta\omega$. For such a consideration, the field amplitude A in the microcavity is given by the relationship

$$A = \frac{\imath E\,\Delta\omega\sqrt{Q}}{\omega_0 - \omega + \imath\Delta\omega} \quad Q \equiv \frac{\omega}{\Delta\omega}, \tag{2}$$

where E and ω are the field amplitude and frequency of optical oscillations in the probe beam, and the quantity Q for $\omega \sim \omega_0$ is close to the cavity finesse (we assume that $Q \gg 1$). Amplitude R of the wave reflected from the cavity can be presented as a sum of the amplitude r_tE of the wave reflected from the front mirror (r_t is the reflectivity of the front mirror, $|r_t| \sim 1$) and amplitude tA of the wave coming out of the cavity through the front mirror (t is the transmission coefficient of the front mirror, $|t| \ll 1$): $R = r_tE + tA$. Using Eq. (2), we can express t through the resonant reflectivity of the cavity $r_{res} = R/E|_{\omega=\omega_0}$, which can be easily evaluated experimentally and, for high-Q symmetric cavities, is a small real value $|r_{res}| \ll 1$. Now, for the reflected field, we obtain the relationship $R = r_tE + (r_{res} - r_t)A/\sqrt{Q}$.

A likely reason for optical nonlinearity of our microcavity is the dependence of the refractive index of the inter-mirror gap on the intensity $|A|^2$ of the field in it. In the simplest case, this dependence can be taken into account assuming that the intensity $|A|^2$ affects the eigen-frequency of the cavity ω_0. In our model, we will consider this dependence retarding and comprised of two contributions: fast (Ω_f with characteristic time T_f) and slow (Ω_s, with characteristic time $T_s \gg T_f$)[24]

$$\begin{cases} \omega_0 = \bar{\omega}_0 + \Omega_s + \Omega_f \\ \dot{\Omega}_{s(f)} + \Omega_{s(f)}/T_{s(f)} = \nu_{s(f)}|A|^2. \end{cases} \tag{3}$$

Here, $\bar{\omega}_0$ is the resonant frequency of the cavity in linear regime, ν_f and ν_s are the constants describing the above contributions and characterizing nonlinearity of the cavity. By measuring time and frequencies in the units of $\Delta\omega^{-1}$ and $\Delta\omega$, respectively, and by passing to the dimensionless field amplitude in the cavity $a \equiv A/\sqrt{Q}E$, we can obtain, using Eqs. (2) and (3), the following set of equations, describing dynamics of the nonlinear cavity:

$$\begin{cases} [1 + \imath z]a = 1 \\ z = b - \theta_s - \theta_f \\ \dot{\theta}_{s(f)} + \theta_{s(f)}/\tau_{s(f)} = g_{s(f)}|a|^2 \end{cases}$$

$$g_{s(f)} \equiv \frac{\nu_{s(f)}QE^2}{\Delta\omega^2} \;\; \theta_{s(f)} \equiv \Omega_{s(f)}/\Delta\omega \;\; b \equiv \frac{\omega - \bar{\omega}_0}{\Delta\omega}. \tag{4}$$

Here, $\tau_{s(f)} \equiv \Delta\omega T_{s(f)}$, and the quantity $z = [\omega - \omega_0]/\Delta\omega$ has the sense of cavity detuning dependent on $|a|^2$. When parameters of the oscillator or regime of its excitation change, the field oscillation amplitude in it is established with the characteristic time $\Delta\omega^{-1}$ which we take for unity. For this reason, the set of equations (4) makes sense under the condition $\Delta\omega^{-1} \ll T_{s(f)}$, which we consider to be satisfied. Let us show that the above model of the nonlinear cavity admits existence of self-oscillation. For this purpose, consider behavior of the cavity in the time scale substantially exceeding T_f. This allows us to consider the fast contribution Ω_f as inertialess, to assume that $\theta_f = c|a|^2$ (where $c \equiv g_f\tau_f$), and to transform the set of equations (4) to the following form:

$$\begin{cases} [1 + z^2]|a|^2 = 1 \\ z = b - \theta_s - c|a|^2 \\ \dot{\theta}_s + \theta_s/\tau_s = g_s|a|^2. \end{cases} \tag{5}$$

From the first two equations, we can express $|a|^2$ through θ_s. Since the dependence $|a|^2(\theta_s)$ is obtained from solution of a cubic equation, it may be multi-valued. It can be confirmed by graphic analysis of the equation for the detuning z (with which the quantity $|a|^2$ is connected as $|a|^2 = [1 + z^2]^{-1}$), whose solution corresponds to the points of crossing of the Lorentzian $y(z) = c/[1 + z^2]$ and straight line $y(z) = b - \theta_s - z$.[27] If the Lorentzian amplitude c is small enough, the equation for the detuning has a single real root $z_1 \approx b - \theta_s$. It can be shown that at $c > c_{cr}$, there appears an interval of values θ_s, for which the equation for detuning has three real roots z_1, z_2, and z_3. Therefore, at $c > c_{cr}$ (below, we assume that $c > 0$), the dependence $|a|^2(\theta_s)$ becomes locally multi-valued and, in the above interval of θ_s, has an S-wise shape (see Fig. 6, in which this interval corresponds to $\theta_s \in [\theta_l, \theta_r]$). With decreasing c, the region of nonuniqueness decreases and, at $c = c_{cr}$ vanishes ($\theta_l = \theta_r|_{c=c_{cr}}$).

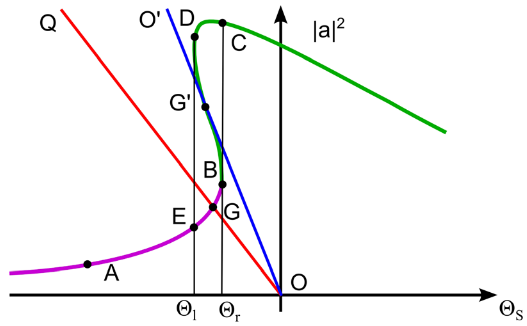

FIG. 6. The S-shaped curve illustrating instability of the nonlinear oscillator.

Using the dependence $|a|^2(\theta_s)$ presented in Fig. 6, we can study, in great detail, dynamics of the considered model of nonlinear cavity. The point on the plane $|a|^2, \theta_s$ that depicts the state of the cavity at arbitrary instant ("mapping point") should necessarily lie on the S-shaped curve (Fig. 6)—in this case, two first equations of system (5) will be satisfied. The character of motion of the mapping point *along* this curve is governed by the third equation of system (5) and represents approaching of this point to the point of crossing of the S-shaped curve and the straight line $|a|^2 = \theta_s/g_s\tau_s$. This point corresponds to a stationary state of the system. There are two essentially different modes of the motion. The first one is realized when the straight line $|a|^2 = \theta_s/g_s\tau_s$ is arranged like the line OQ (Fig. 5). In this case, the mapping point, by moving from the initial point A along the S-shaped curve to the right, comes to the stationary point G and stays there infinitely long. The second mode of the motion is realized when, for the given parameters of the system, the straight line $|a|^2 = \theta_s/g_s\tau_s$ intersects the S-shaped curve in some point G' at the return segment of the interval of non-uniqueness BD (as, e.g., the line OO' in Fig. 5). In this case, the mapping point, when moving from the point A of the S-shaped curve towards the stationary point G', will come to point B where switching to point C will occur. After that, the mapping point will start moving towards the stationary point G' over the segment CD, and at point D a step-wise switching to point E will occur again, and so on. Thus, in the case of the second mode of motion, the mapping point performs periodic motion over the loop $EDCB$ (Fig. 6) formed by two vertical tangents DC and CB to the S-shaped curve and by two segments EB and DC. It is seen from Fig. 6 that, to obtain such an instable (self-oscillatory) regime at $c > 0$, G_s should be negative (in the general case, the constants c and g_s (g_f and g_s) should have different signs). The third equation of system (5) can be written in the form $\dot{\theta}_s = g_s\,|a|^2(\theta_s) - \theta_s/\tau_s$, wherefrom we obtain the following expressions for the dimensionless times τ_{EB} (τ_{DC}), during which the mapping point passes the path EB (DC), and for the total period τ_A of the self-oscillation

$$\tau_{EB(DC)} = \left| \int_{EB(DC)} \frac{d\theta_s}{g_s|a|^2(\theta_s) - \theta_s/\tau_s} \right| \tau_A = \tau_{EB} + \tau_{DC}. \tag{6}$$

The multi-valued dependence $a^2(\theta_s)$ (Fig. 6), entering these equations, can be obtained both numerically and analytically using the Cardano formula. Calculations according Eq. (6) have shown that the period of self-oscillations substantially depends on the intensity-related parameters of the problem c and g_s and may be an order of magnitude smaller than τ_s. Thus, the above consideration seems quite plausible in the case when τ_s exceeds τ_f by more than an order of magnitude.

Summarizing consideration of the self-oscillatory regime in the above model of nonlinear cavity, let us enumerate the main conditions of the self-excitation. (i) $|c| > c_{cr} = 8\sqrt{3}/9$. The sense of this condition is that intensity $|A|^2$ of the field in the cavity should be high enough to provide the nonlinear shift of the cavity eigen-frequency of the order of the resonance width $\Delta\omega$.[28] (ii) The line $|a|^2 = \theta_s/g_s\tau_s$ should intersect the S-shaped curve at the return path of the ambiguity region. Note that the relative position of the above line and S-shaped curve depends on the dimensionless static detuning b. By varying this quantity, one can remove the system from the regime of self-oscillations.

Let us pass now to consideration of the cavity response to a small modulation of the detuning δb in the pre-threshold regime, when $c < c_{cr}$. In this regime, the system of equations (6) has a stable stationary solution (we denote it a_0, z_0, θ_{s0}, θ_{f0}) that is obtained from Eq. (6) by ignoring the terms $\dot{\theta}_s$ and $\dot{\theta}_f$. The problem we are interested in can be now formulated as follows. Let us make in Eq. (6) the substitution $b \to b + \delta b(t)$, $\delta b/b \ll 1$ and find response δr of the microcavity reflectivity in the vicinity of the stationary solution of Eq. (6) to a small modulation of the detuning δb. In conformity with the standard procedure, one has to present the sought solution of Eq. (6) in the form $a(t) = a_0 + \delta a(t), z(t) = z_0 + \delta z(t), \theta_s(t) = \theta_{s0} + \delta\theta_s(t), \theta_f(t) = \theta_{f0} + \delta\theta_f(t)$ and to find the values δa, δz, $\delta\theta_s$, $\delta\theta_f$ in the first perturbation order in δb. It is expedient to perform the calculations for the quantities $q \equiv 2\mathrm{Re}\,[\delta a a_0^*]$ and $v \equiv 2\mathrm{Im}\,[\delta a a_0^*]$, entering the expression for variations of the cavity reflectivity as follows: $\delta r = (r_{res} - r_t)[q + \imath v]/2a_0^*$. If the time dependence of δb is described by harmonic oscillations with the frequency ν, then, for the amplitudes of oscillations of the quantities q and v (denote them by q_0 and v_0), we obtain the following equations:

$$|v_0| = |\chi(\nu)\delta b| \quad |q_0| = |z_0\chi(\nu)\delta b|, \tag{7}$$

where the *susceptibility* $\chi(\nu)$ is defined as

$$\chi(\nu) = \frac{2}{\left[1 + z_0^2\right]^2 - 2z_0\left[g_f\tau_f/(1 - \imath\nu\tau_f) + g_s\tau_s/(1 - \imath\nu\tau_s)\right]}. \tag{8}$$

The steady-state value of the detuning z_0 entering these formulas can be found from the equation

$$b - z_0 = \frac{g_f\tau_f + g_s\tau_s}{1 + z_0^2}, \tag{9}$$

which, in the considered stable regime of the cavity, has a single real solution. Using the expression for susceptibility

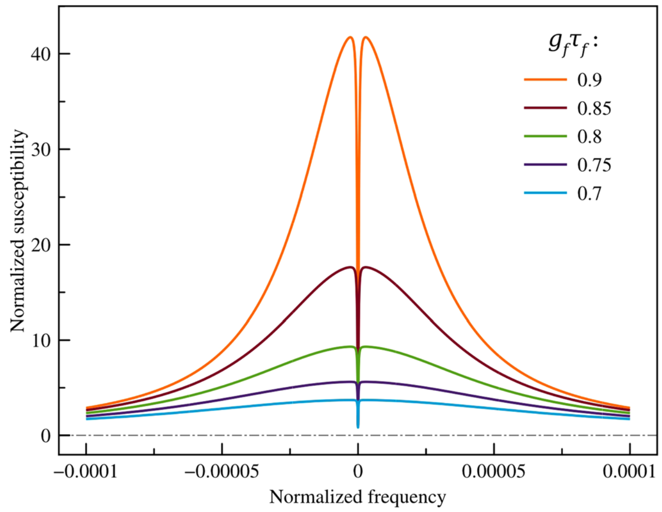

FIG. 7. Frequency dependence of the susceptibility (8) normalized to the linear susceptibility $|\chi(\nu, c)\,(1 + b^2)^2|^2$, at $c = g_f\tau_f = 0.7$, 0.75, 0.8, 0.85, and 0.9. The values of other parameters are: $b = 1$, $\tau_s = 2 \times 10^7$, $\tau_f = 0.0002\,\tau_s$, and $g_s = -0.6\,c/\tau_s$.

(8), we can calculate its behavior upon approaching to the instability threshold $c \to c_{cr}$. From the results of such calculations presented in Fig. 6, we can see that the amplitude of the susceptibility $\chi(\nu)$ (and, hence, the amplitude of the reflectivity modulation δr) substantially increases at $c \to c_{cr}$, and the shape of its frequency dependence (excluding a narrow dip at $\nu = 0$) qualitatively coincides with that for the gain factor in Eq. (1). The widths of the main peak and the central narrow dip of the function $|\chi(\nu)|^2$ are controlled by the times τ_f and τ_s (Fig. 7).

Thus, the main qualitative properties of a real microcavity (listed at the beginning of this section) are successfully described by our model. For this reason, a more detailed analysis of the model (which seems quite realistic) is now not needed, and we will restrict ourselves to two remarks. First, the appearance of a narrow central dip in the function $|\chi(\nu)|^2$ is a consequence of the condition necessary for the self-excitation $g_f g_s < 0$ and, for this reason, this dip probably is physically meaningful.[29] Second, our assumptions about presence of fast and slow response of the refractive index to variations of the light beam intensity do not seem unrealistic: the former can be related to bleaching of the QW exciton susceptibility,[30] while the latter, with relatively slow variations of the photo-induced charge or temperature.[19,20]

VI. CONCLUSIONS

We studied properties of the Kerr rotation noise in the light beam reflected from a Bragg microcavity with a quantum well in its inter-mirror gap. In the spectral region corresponding to anti-crossing of the exciton-polariton branches, we have found a dramatic enhancement (by more than a factor of 300) of the noise signal. The accumulation time, in our experiments, is less than 1 s, which allows us to observe the noise signal in real time. The effect is interpreted in terms of a strong increase of polarimetric sensitivity of the nonlinear microcavity in the vicinity of the threshold of self-oscillations. In the framework of the developed model, we have described the main features of the noise signals also in the case of negative detuning of the photon mode. The effect of nonlinear amplification with the intensity-controlled gain factor, described in this paper, provides possibility to strongly improve sensitivity of the microcavity reflectivity to variations of the intermirror gap refractive index highly interesting for the spin noise spectroscopy and for solving other problems of detecting weak polarization signals.

ACKNOWLEDGMENTS

Financial support from the Ministry of Education and Science of the Russian Federation (Contract No. 11.G34.31.0067), Saint Petersburg State University (Grant No. 11.38.213.2014), and the Russian Foundation for Basic Research and the Deutsche Forschungsgemeinschaft in the frame of International Collaborative Research Center TRR 160 (Project No. 15-52-12013) is acknowledged. A.V.K. acknowledges support from the EPSRC Established Career Fellowship (Grant No. RP008833).

The work was carried out using the equipment of SPbU Resource Center "Nanophotonics" (photon.spbu.ru).

[1]V. S. Zapasskii, Adv. Opt. Photon. **5**, 131–168 (2013).
[2]E. B. Aleksandrov and V. S. Zapasskii, J. Exp. Theor. Phys. **54**, 64–67 (1981).
[3]S. A. Crooker, D. G. Rickel, A. V. Balatsky, and D. Smith, Nature **431**, 49 (2004).
[4]T. Mitsui, Phys. Rev. Lett. **84**, 5292 (2000).
[5]G. M. Müller, M. Oestreich, M. Römer, and J. Hubner, Physica E **43**, 569 (2010).
[6]M. Römer, J. Hübner, and M. Oestreich, Rev. Sci. Instrum. **78**, 103903 (2007).
[7]P. Glasenapp, A. Greilich, I. I. Ryzhov, V. S. Zapasskii, D. R. Yakovlev, G. G. Kozlov, and M. Bayer, Phys. Rev. B **88**, 165314 (2013).
[8]T. Mitsui and K. Aoki, e-print arXiv:1309.3097v1 [physics.atom-ph].
[9]S. Starosielec and D. Hägele, Appl. Phys. Lett. **93**, 051116 (2008).
[10]F. Berski, H. Kuhn, J. G. Lonnemann, J. Hübner, and M. Oestreich, Phys. Rev. Lett. **111**, 186602 (2013).
[11]G. M. Müller, M. Römer, J. Hübner, and M. Oestreich, Phys. Rev. B **81**, 121202(R) (2010).
[12]S. A. Crooker, J. Brandt, C. Sandfort, A. Greilich, D. R. Yakovlev, D. Reuter, A. D. Wieck, and M. Bayer, Phys. Rev. Lett. **104**, 036601 (2010).
[13]R. Dahbashi, J. Hübner, F. Berski, K. Pierz, and M. Oestreich, e-print arXiv:1306.3183v2 [cond-mat.mes-hall].
[14]G. M. Muller, M. Romer, D. Schuh, W. Wegscheider, J. Hubner, and M. Oestreich, Phys. Rev. Lett. **101**, 206601 (2008).
[15]S. V. Poltavtsev, I. I. Ryzhov, M. M. Glazov, G. G. Kozlov, V. S. Zapasskii, A. V. Kavokin, P. G. Lagoudakis, D. S. Smirnov, and E. L. Ivchenko, Phys. Rev. B **89**, 081304(R) (2014); arXiv:1311.6587v1 [cond-mat.mes-hall].
[16]A. Kavokin, J. J. Baumberg, G. Malpuech, and F. P. Laussy, *Microcavities* (Clarendon Press, Oxford, 2006).
[17]R. Rapaport, E. Cohen, A. Ron, E. Linder, and L. N. Pfeiffer, Phys. Rev. B **63**, 235310 (2001).
[18]S. V. Poltavtsev, I. I. Ryzhov, R. V. Cherbunin, A. V. Mikhailov, N. E. Kopteva, G. G. Kozlov, K. V. Kavokin, V. S. Zapasskii, P. V. Lagoudakis, and A. V. Kavokin, Phys. Rev. B **89**, 205308 (2014).
[19]H. M. Gibbs, *Optical Bistability: Controlling Light with Light* (Academic Press, Inc. and Harcourt Brace Jovanovich Publishers, Orlando, 1985).
[20]S. L. McCall, Appl. Phys. Lett. **32**, 284 (1978).
[21]J. L. Jewell, H. M. Gibbs, S. S. Tarng, A. C. Gossard, and W. Wiegmann, Appl. Phys. Lett. **40**, 291 (1982).
[22]A. Baas, J. P. Karr, H. Eleuch, and E. Giacobino, Phys. Rev. A **69**, 023809 (2004).
[23]A. Baas, J.-Ph. Karr, M. Romanelli, A. Bramati, and E. Giacobino, Phys. Rev. B **70**, 161307(R) (2004).
[24]Such a mechanism of optical nonlinearity leading to regenerative oscillations of the cavity was described in Refs. 20 and 21.
[25]The interpretation presented below is not the only one. In particular, the nonmagnetic peak of the noise spectrum that was considered in Ref. 15 to be a result of the spin-spin electron-nuclear interaction. In our opinion, the hypothesis of built-in amplifier explains the giant noise observed in the present work (in the region of anti-crossing) and the bimodal structure of the noise spectrum (in the region of the negative detuning) in the most plausible way.
[26]Dependence of this kind follows from the model described in Sec. IV.
[27]These dependences are plotted on the *yz*-plane.
[28]Note that for the spectra of Fig. 4, in the region of anti-crossing of the polariton branches, conditions of this kind (at least qualitatively) appear to be met.
[29]In our experiments, observation of the noise spectra in the frequency range below 2 MHz was hampered by high level of intrinsic noise of the spectrum analyzer.
[30]R. Houdre, J. L. Gibernon, P. Pellandini, R. P. Stanley, U. Oesterle, C. Weisbuch, J. O'Gorman, B. Roycroft, and M. Ilegems, Phys. Rev. B **52**, 7810 (1995).